ERDC/GRL TR-22-2

Geospatial Research Laboratory

US Army Corps
of Engineers®
Engineer Research and
Development Center

ERDC
ENGINEER RESEARCH & DEVELOPMENT CENTER

Analysis of Spectropolarimetric Responses in the Visible and Infrared for Differentiation between Similar Materials

Sarah J. Becker, Heather S. Sussman, S. Bruce Blundell,
Vern C. Vanderbilt, and Igor Semyonov

September 2022

The US Army Engineer Research and Development Center (ERDC) solves the nation's toughest engineering and environmental challenges. ERDC develops innovative solutions in civil and military engineering, geospatial sciences, water resources, and environmental sciences for the Army, the Department of Defense, civilian agencies, and our nation's public good. Find out more at www.erdc.usace.army.mil.

To search for other technical reports published by ERDC, visit the ERDC online library at https://erdclibrary.on.worldcat.org/discovery.

ERDC/GRL TR-22-2
September 2022

Analysis of Spectropolarimetric Responses in the Visible and Infrared for Differentiation between Similar Materials

Sarah J. Becker, Heather S. Sussman, S. Bruce Blundell, Vern C. Vanderbilt, Igor Semyonov

US Army Engineer Research and Development Center (ERDC)
Geospatial Research Laboratory (GRL)
7701 Telegraph Road
Alexandria, VA 22315-3864

Final Report

Prepared for Headquarters, US Army Corps of Engineers
Washington, DC 20314-1000

Under PE 611102 / AB2

Abstract

Spectropolarimetric research has focused on target detections of materials that have a high degree of contrast from background materials, such as identification of a manmade object embedded in a vegetative background. This study presents an approach using spectropolarimetric imagery in visible, shortwave infrared, and longwave infrared bands to differentiate between similar natural and manmade materials. The method employs Michelson contrast and Kruskal-Wallis one-way analysis of variance (ANOVA) H-test to determine if a distinction can be found in pairwise comparisons of similar and different materials using the Stokes parameters in the visible, shortwave infrared, and longwave infrared bands. Results showed that similar natural and manmade materials were differentiable in spectropolarimetric imagery using the Michelson contrast and ANOVA. This approach provides a way to use spectropolarimetric imagery to distinguish between materials that are similar to each other.

Contents

Figures and Tables

Figures

Tables

Preface

This study was conducted for the U.S. Army Corps of Engineers under PE 611102, Project AB2.

The work was performed by the Data and Signature Analysis Branch of the Topography, Imagery and Geospatial Research Division, US Army Engineer Research and Development Center (ERDC), Geospatial Research Laboratory (GRL). At the time of publication, Austin Davis was Technical Director, Jennifer Smith was Branch Chief, and Jeffrey Murphy was Division Chief. The Deputy Director and Acting Director of ERDC-GRL was Valerie Carney.

The authors thank Frank Pantuso, Collin Bright, and Jerome Zadnik from the United States Army Command, Control, Communication, Computers, Cyber, Intelligence, Surveillance and Reconnaissance Center Research and Technology Integration Directorate and Jean Nelson and Kristofer Lasko from ERDC for scientific discussion and guidance.

COL Christian Patterson was Commander of ERDC, and Dr. David W. Pittman was the Director.

Acronyms and Abbreviations

ANOVA	analysis of variance
AOP	angle of polarization
DOLP	degree of linear polarization
ETM	enhanced thermal
LWIR	longwave infrared
ROI	regions of interest
SWIR	shortwave infrared
VIR	visible and infrared
VIS	visible

This page intentionally left blank.

1 Introduction

Distinguishing between similar materials in imagery is challenging as they may exhibit nearly identical spectral signatures (Becker et al. 2018; Herold et al. 2002). Prior research has investigated use of polarimetric imagery to distinguish between manmade materials from natural backgrounds (Bright, Pantuso, and Zadnik 2019; Pantuso et al. 2018), but has not focused on distinguishing between similar materials. This research effort investigates the phenomenology of the polarimetric responses and spectral energy interactions with materials in both the natural and built environment. We will explore this interaction through analysis of multiband field data of various materials that provide spectropolarimetric signatures in the visible and infrared (VIR) region of the electromagnetic spectrum. Techniques to distinguish material pairs will better inform future research in image science, material recognition, and land cover mapping.

1.1 Objectives

The objective of this research is to discover the most effective characterization of subsets of VIR bands to the energy interaction with materials. This project will achieve this by investigating the phenomenology of spectropolarimetric responses and with materials in both the natural and built environment. Multiband VIR spectropolarimetric imagery provide a capability to better characterize materials in imagery, especially in situations where the materials are similar to the background or other objects in the imagery.

1.2 Approach

This research will test whether the interaction of spectral energy with commonly encountered material objects creates spectropolarimetric responses that can be attributed, optimized, and segmented into separable material subsets. The approach will fuse polarimetric signature responses in two-dimensional imagery for VIR spectropolarimetric responses and determine if the responses are separable using multivariate statistics

1.3 Scope

Previous research has applied spectropolarimetric imagery to find manmade materials among natural backgrounds. This research expands by using spectropolarimetric imagery captured with sensors developed for ERDC to distinguish similar materials from each other.

1.4 Background

Multispectral sensor systems measure the intensity of reflected radiation from materials in a scene across a number of bands. Traditional spectral-based remote sensing techniques may not be able to distinguish materials in a scene when those materials exhibit similar spectral signatures (Myint et al. 2011). Other remote sensing approaches, such as the use of hyperspectral, improve material identification, but are costly and still do not enable identification of materials when they are spectrally similar to other materials.

In electromagnetic wave theory, light is described as the propagation of energy due to constantly varying electric and magnetic fields. These fields can be represented as vectors existing in the plane perpendicular to the direction of propagation. When natural light strikes a non-metallic surface, there is a preferential reflection for those waves for which the electric field vector is vibrating parallel to the surface, resulting in linear polarization of the reflected beam (Figure 1). In addition, for emissive band infrared (>3 microns), an emission component exists. This results in a very strong polarization signal when the reflected component is small (Pantuso et al. 2018). Polarization may provide clues about the feature, such as shape, roughness, or other surface patterns. Polarized imagery shows the distribution of the polarization state across the entire scene from a variety of materials and objects.

Figure 1. Polarization from surface reflectance.

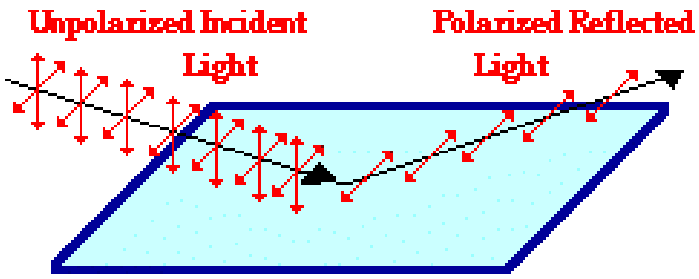

Spectropolarimetric data collection in the VIR region uses both unpolarized and polarimetric information to identify materials in a scene. Research is exploring ways to exploit these data and has focused on spectropolarimetric sensors with one band or with target materials that contrast from background materials (Gurton and Felton 2009; Zhao et al. 2009).

Unpolarized light incident on a material is reflected, absorbed, and transmitted at the material surface. Surface reflectance is the incident light that bounces off the surface of a material when the surface modifies the polarization of the incident light and never interacts with the molecular structure of that material. The surface-reflected light, if the surface is even somewhat smooth, will be partially polarized; polarized reflectance will be largely spectrally invariant. Conversely, the transmitted light interacts with the volume of the material, where it is both scattered and absorbed. The light scattered from the material volume back through the material surface is the non-polarized material volume reflectance, which displays the spectral absorption characteristics of the material.

All materials exhibit some amount of surface reflectance and some amount of volume reflectance. Many materials display volume reflectance with varying degrees of spectral variance. Figure 2 shows volume reflectance spectra in the visible (VIS) and shortwave infrared (SWIR) for four common substances: concrete, black paint, grass, and pine wood. The curves for concrete and black paint are primarily spectrally flat. In contrast, the curves for living vegetation have a high degree of spectral variance. While the polarized surface reflectance of a green leaf is spectrally flat and displays no evidence of chlorophyll pigments, the non-polarized volume reflectance displays pronounced evidence of chlorophyll pigments through differential absorption. Consideration of the polarized component of surface reflectance from a leaf may provide additional information, such as its surface roughness. The same holds true for other substances and may allow materials with similar spectrally flat volume reflectances to become separable through their polarimetric signatures. These two reflectances, while linked mathematically, are essentially unrelated to each other. When analyzed together, they may be used to provide additional information to help distinguish materials.

Figure 2. Spectral reflectance of different materials (natural and manmade).

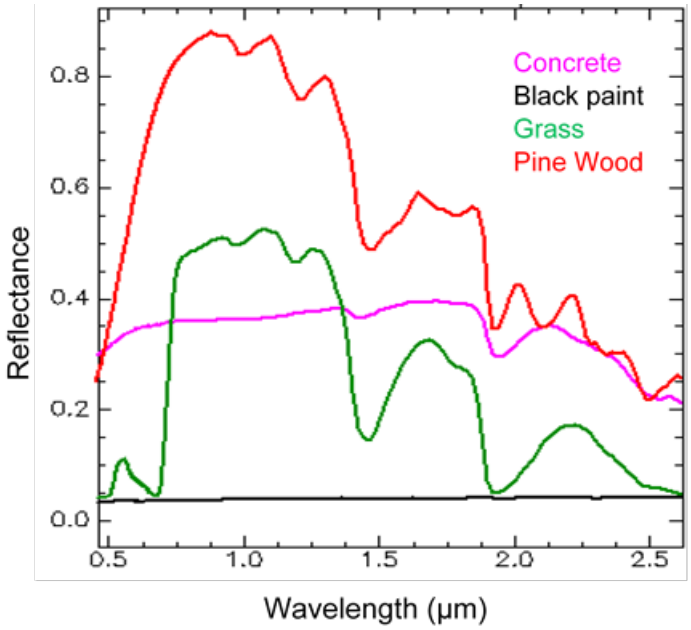

Traditionally, polarimetric measurements are taken in one band of the VIS, SWIR, or longwave infrared (LWIR), and research has shown benefits and shortcomings for each. Prior spectropolarimetric research outside of ERDC focused on using single spectropolarimetric band imagery to characterize ground features or on multiband imagery to examine single land covers (Gurton and Felton 2009; Zhao et al. 2009). The United States Army Command, Control, Communication, Computers, Cyber, Intelligence, Surveillance and Reconnaissance Center Research and Technology Integration Directorate considered the VIS, SWIR, and LWIR bands separately to investigate small manmade material detection in cluttered imagery suppressing the clutter to cue potential threats (Bright, Pantuso, and Zadnik 2019; Pantuso et al. 2018). Most research has focused on using polarization to detect manmade materials (Lavigne et al. 2009). However, NASA and USDA researchers applied hyperspectral spectropolarimetry to remove the surface reflection and better study leaf photochemical effects evident in the material reflection (Vanderbilt, Daughtry, and Dahlgren 2019).

Spectropolarimetric remote sensing uses Stokes parameters and other mathematical metrics derived from measurements captured by polarimetric cameras to differentiate between materials. The Stokes parameters are denoted using the terms S0, S1, S2, and S3. They form a

one-dimensional array that describes the polarization of light based on its time-averaged intensity contained in different polarization states (Tyo et al. 2006). S0 measures unpolarized light and is analogous to how a panchromatic would be represented. S1, S2, and S3 are the polarimetric Stokes parameters. S1 measures the amount of linearly polarized light that passes through a vertical or horizontal filter, and S2 measures diagonally polarized light that passes through a diagonal filter (Table 1). S3 measures circularly polarized light and is usually ignored because circular polarization is rare in nature although more common in urban settings (Können 1985). S3 was not used in this research.

Table 1. Definition of the Stokes parameters.

Stokes parameter	Polarization State
$S0 = I_{0^\circ} + I_{90^\circ}$	Unpolarized
$S1 = I_{0^\circ} - I_{90^\circ}$	Transmits only light polarized at linear horizontal (0°) or linear vertical (90°) component
$S2 = I_{45^\circ} - I_{45^\circ}$	Transmits only linear +45° or linear −45°

The degree of linear polarization (DOLP), angle of polarization (AOP), and enhanced thermal (ETM) are the derived polarimetric Stokes parameters. The DOLP and AOP are other mathematical equations employed in spectropolarimetry that are products of the Stokes parameters. The DOLP expresses the amount of linearly polarized light as a fraction of the total amount of reflected light, and AOP is the angle of polarization at which light that is reflected from the surface is linearly polarized. The ETM is a technique developed by Polaris Sensor Technologies Inc. of Huntsville, AL (hereafter "Polaris"), to combine polarization information for the purpose of visualization (Chenault et al. 2015). The technique uses the hue, saturation, value method to display the colorized image. Hue is the AOP, saturation is the DOLP, and value is the unpolarized intensity image, S0. All these quantities help distinguish polarized materials in a scene.

$$\mathbf{DOLP} = \frac{\sqrt{\boldsymbol{S1}^2 + \boldsymbol{S2}^2}}{\boldsymbol{S0}}$$

$$\mathbf{AOP} = \frac{\mathbf{1}}{\mathbf{2}}\mathbf{arctan}\left(\frac{\boldsymbol{S1}}{\boldsymbol{S2}}\right)$$

Previous research (supported by the US military) on polarimetric effects from materials outside of the microwave band has been largely concerned with isolating individual objects from a natural or cluttered background. This effort focuses on creating strategies to characterize patterns of materials in a more complex urban setting using a multiband spectropolarimetric approach.

2 Methodology

This study seeks an understanding of the fundamental spectropolarimetric interaction of VIR energy with common natural and manmade materials and how this interaction can be optimized for the differentiation of these materials.

2.1 Data

The researchers exploited overhead imagery collected over Spanish Fork, UT, and Grand Junction, CO, on June 25 and 26, 2019. The data are composed of unpolarized and polarimetric reflectance values in the VIS, SWIR, and LWIR. Polaris collected the overhead data using a suite of cameras it developed for the U.S. Army Engineer Research and Development Center (ERDC), Geospatial Research Laboratory (GRL) (Roche and Pezzaniti 2019) (see Table 2, Figure 3, and Figure 4).

Table 2. Spectropolarimetric camera specifications developed by Polaris Sensor Technologies, Inc.

-	VIS camera	SWIR camera	LWIR camera
Wavelength (μm)	0.4-0.7	1.1-1.7	7.5-13.5
Polarization States	S0, S1, S2	S0, S1, S2	S0, S1, S2

Figure 3. Spectropolarimetric cameras (VIS, SWIR, and LWIR) developed for GRL to collect imagery of study sites.

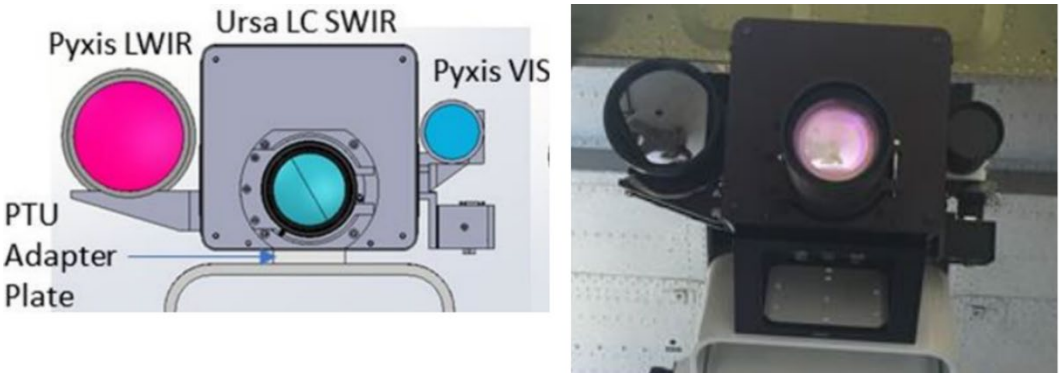

Figure 4. Imagery matrix showing spectropolarimetric (VIS, SWIR and LWIR) imagery, representing three different polarimetric states (S0, S1, and S2). The scene is of St. Mary's Hospital, Grand Junction, CO.

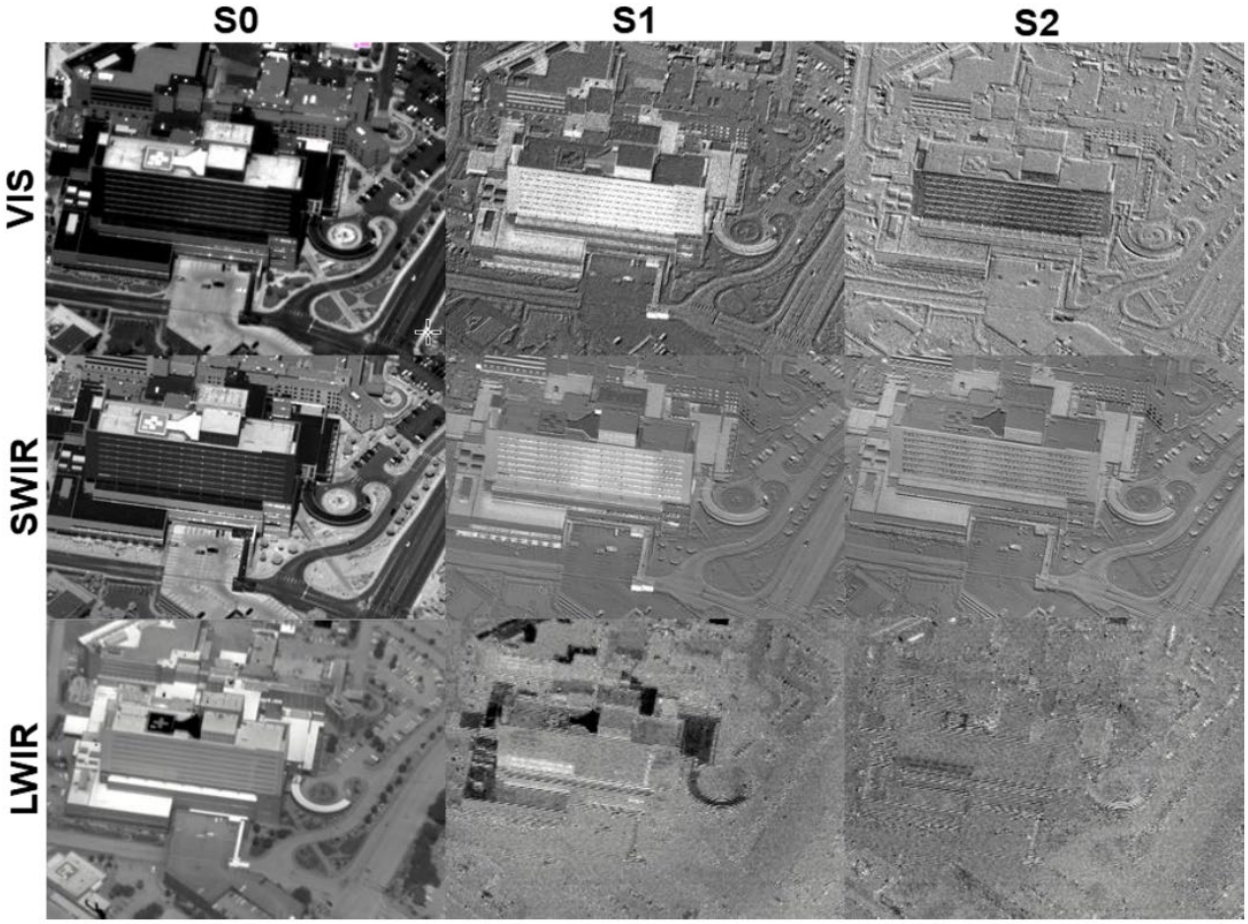

Polaris conducted multiple flyovers at each study site. Data were taken on days with a clear sky as SWIR sky illumination is known to vary on partly cloudy days and may impact results. We selected two flyovers at each study site. Each flyover captured hundreds of frames of the area, from which we selected two. Since we collected imagery in the VIS, SWIR, and LWIR, the imagery we analyzed totaled 24 frames. Polaris developed software that extracted the VIS, SWIR, and LWIR values for the S0, S1, and S2 Stokes parameters from the imagery and derived the DOLP, AOP, and ETM from the Stokes parameters for each band. We ingested the imagery into the software, identified materials for further analysis, and created polygon regions of interest (ROI) around materials to obtain the values for all of the parameters (Figure 5). We input the values into spreadsheets for further analysis.

Figure 5. Polaris software was used to draw polygons around each item of interest. The software extracted descriptive statistics for each Stokes parameter at each band.

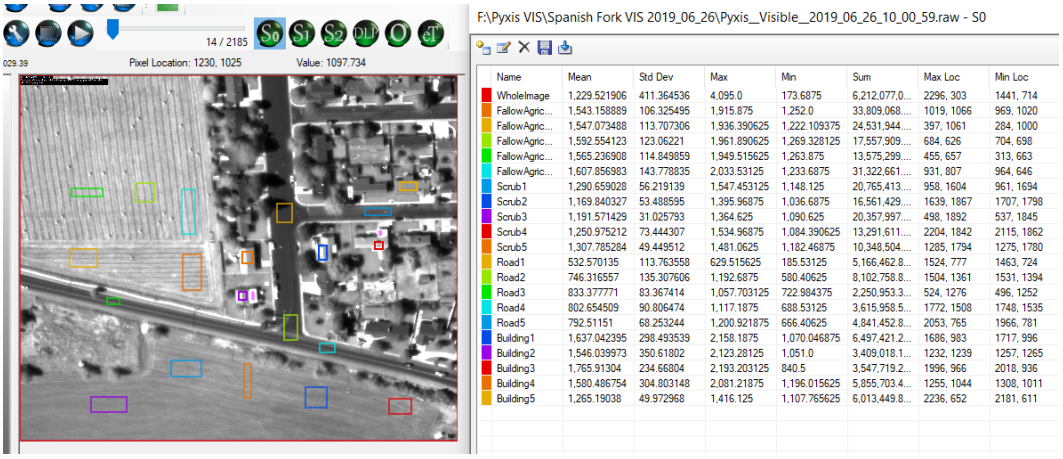

Name	Mean	Std Dev	Max	Min	Sum	Max Loc	Min Loc
WholeImage	1,229.521906	411.364536	4,095.0	173.6875	6,212,077,0...	2296, 303	1441, 714
FallowAgric...	1,543.158889	106.325495	1,915.875	1,252.0	33,809,068....	1019, 1066	969, 1020
FallowAgric...	1,547.073488	113.707306	1,936.390625	1,222.109375	24,531,944....	397, 1061	284, 1000
FallowAgric...	1,592.554123	123.06221	1,961.890625	1,269.328125	17,557,909....	684, 626	704, 698
FallowAgric...	1,565.236908	114.849859	1,949.515625	1,263.875	13,575,299....	455, 657	313, 663
FallowAgric...	1,607.856983	143.778835	2,033.53125	1,233.6875	31,322,661....	931, 807	964, 646
Scrub1	1,290.659028	56.219139	1,547.453125	1,148.125	20,765,413....	958, 1604	961, 1694
Scrub2	1,169.840327	53.488595	1,395.96875	1,036.6875	16,561,429....	1639, 1867	1707, 1798
Scrub3	1,191.571429	31.025793	1,364.625	1,090.625	20,357,997....	498, 1892	537, 1845
Scrub4	1,250.975212	73.444307	1,534.96875	1,084.390625	13,291,611....	2204, 1842	2115, 1862
Scrub5	1,307.785284	49.449512	1,481.0625	1,182.46875	10,348,504....	1285, 1794	1275, 1780
Road1	532.570135	113.763558	629.515625	185.53125	5,166,462.8...	1524, 777	1463, 724
Road2	746.316557	135.307606	1,192.6875	580.40625	8,102,758.8...	1504, 1361	1531, 1394
Road3	833.377771	83.367414	1,057.703125	722.984375	2,250,953.3...	524, 1276	496, 1252
Road4	802.654509	90.806474	1,117.1875	688.53125	3,615,958.5...	1772, 1508	1748, 1535
Road5	792.51151	68.253244	1,200.921875	666.40625	4,841,452.8...	2053, 765	1966, 781
Building1	1,637.042395	298.493539	2,158.1875	1,070.046875	6,497,421.2...	1686, 983	1717, 996
Building2	1,546.039973	350.61802	2,123.28125	1,051.0	3,409,018.1...	1232, 1239	1257, 1265
Building3	1,765.91304	234.66804	2,193.203125	840.5	3,547,719.2...	1996, 966	2018, 936
Building4	1,580.486754	304.803148	2,081.21875	1,196.015625	5,855,703.4...	1255, 1044	1308, 1011
Building5	1,265.19038	49.972968	1,416.125	1,107.765625	6,013,449.8...	2236, 652	2181, 611

2.2 Statistical methods

We investigated and quantified spectropolarimetric reflectance for different materials in the overhead imagery with a focus on differentiating between manmade and natural materials. Relationships were defined among polarization states and received intensity for each material in each band. We investigated techniques to differentiate between the materials. These techniques included multi-image manipulation processes such as band ratioing using the Michelson contrast equation, exploratory analysis using box and whisker plots, and statistical analysis using Kruskal-Wallis analysis of variance (ANOVA).

2.2.1 Michelson contrast

The Michelson contrast equation (Michelson 1927) compares two materials to each other. The equation is a simple normalized difference contrast where the mean of one material is subtracted from the mean of a second material divided by the sum of the two. This approach assumes the materials tested have relatively uniform responses.

$$\text{Michelson Contrast} = \frac{\text{mean(material 1)} - \text{mean(material 2)}}{\text{mean(material 1)} + \text{mean(material 2)}}$$

The Michelson contrast equation was employed to determine whether the polarimetric and derived Stokes parameters—S1, S2, DOLP, AOP, and ETM—provide additional information beyond what the unpolarized S0 Stokes parameter provides in differentiating between similar materials.

Traditional remote sensing has relied on spectral data, which are equivalent to what the combined S0, S1, and S2 capture, to identify and map features in imagery. This research effort adds polarimetric and derived data to determine their utility in distinguishing between materials that are indistinguishable in the unpolarized state.

Pairwise comparisons were calculated using same and different materials in imagery and in order to test whether the unpolarized parameter differed from the polarimetric parameters (Table 3). Specifically, we used the Michelson contrast to test whether the unpolarized S0 contrast medians are distinct from the S1, S2, DOLP, AOP, and ETM polarization and derived parameter medians. The S0 Stokes parameter represents unpolarized panchromatic intensity and the other Stokes and derived parameters are based on polarimetric responses. We chose a test based on Michelson contrasts to demonstrate multiband spectropolarimetric techniques. Multiband spectral reflectance satellites are already commonly used (e.g., WorldView and Landsat sensors), while multiband spectropolarimetric satellites have not yet been deployed.

Table 3. Michelson Contrast (in the green highlighted column) computed for mean values (in red boxes) of each parameter. This example shows cars vs. cars and cars vs. buildings; however, the Michelson Contrast was calculated for all feature combinations.

Target description	Mode	Mean value	Mean for whole image	Standard deviation	S.D. for whole image	Min Value	M1: Cm Mi
Car1	S0	6939.451660	4082.397436	2779.343296	1022.148214	2860.131836	0.095965
Car2	S0	5724.181274	4082.397436	1453.679809	1022.148214	3725.952148	
Car1	S1	0.061016	0.029071	0.001342	0.021852	0.059565	0.013597
Car2	S1	0.059379	0.029071	0.000645	0.021852	0.058296	
Car1	S2	0.051767	0.021693	0.07865	0.019263	-0.039238	-0.12765
Car2	S2	0.066917	0.021693	0.083327	0.019263	-0.034167	
Car1	DoLP	0.101641	0.040516	0.047533	0.022863	0.060436	-0.03499
Car2	DoLP	0.109012	0.040516	0.055352	0.022863	0.064788	
Car1	AOP	11.659479	18.115843	19.552998	16.679775	-16.146715	-0.13569
Car2	AOP	15.320343	18.115843	19.305176	16.679775	-14.8304	

Target description	Mode	Mean value	Mean for whole image	Standard deviation	S.D. for whole image	Min Value	M1: Cm Mi
Car1	S0	6939.451660	4082.397436	2779.343296	1022.148214	2860.131836	0.208014
Building1	S0	4549.569535	4082.397436	135.087596	1022.148214	4395.358398	
Car1	S1	0.061016	0.029071	0.001342	0.021852	0.059565	0.422815
Building1	S1	0.024752	0.029071	0.011451	0.021852	0.001295	
Car1	S2	0.051767	0.021693	0.07865	0.019263	-0.039238	0.489955
Building1	S2	0.017721	0.021693	0.004089	0.019263	0.006503	
Car1	DoLP	0.101641	0.040516	0.047533	0.022863	0.060436	0.52785
Building1	DoLP	0.03141	0.040516	0.00938	0.022863	0.007369	
Car1	AOP	11.659479	18.115843	19.552998	16.679775	-16.146715	-0.253856
Building1	AOP	19.593155	18.115843	7.709174	16.679775	5.707752	

2.2.2 Box-and-whisker plots

The difference between the Michelson contrasts for the S0 and polarized and derived Stokes parameters was examined using box-and-whisker plots

to determine additional information the polarized and derived Stokes parameters provide. The interquartile range is the 25th to 75th percentile (this comprises the boxplot part of the box-and-whisker plot), the median is the middle value of the dataset, the whiskers are 1.5 times IQR plus the 75th or 25th percentile, and the notch is the 95% confidence interval of the median (Figure 6). According to Chambers et al. (1983), the box-and-whisker plot is not a formal statistical test, but if the notches for two variables do not overlap, it is an indicator that the variables may be statistically significantly different at the 95% confidence interval. We are not claiming statistical significance because our sample size is small, but we are using the notch comparison as an exploratory measure to suggest a difference between two materials. For every band, we compared the notches of each box-and-whisker plot between the S0 and polarized Stokes parameters for every material to determine which materials were different from each other.

Additionally, we examined whether the boxplot, excluding whiskers and outliers, overlapped with a Michelson contrast value of zero. A contrast that overlaps with zero shows low to no contrast between materials, indicating either the materials are similar, the same, or are dissimilar materials that are not differentiable in that Stokes parameter.

Figure 6. Box-and-whisker plot with its components labeled and example of non-overlapping notches between two plots indicating the two materials are from different populations.

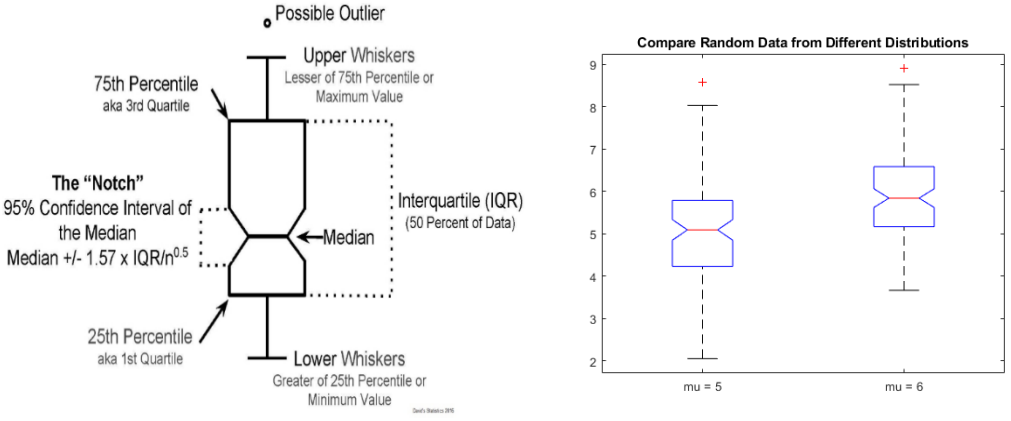

2.2.3 Kruskal-Wallis analysis of variance

We performed pairwise comparisons of materials using the Kruskal-Wallis one-way ANOVA H-test (Kruskal and Wallis 1952). The null hypothesis of this test is that the means of two groups are identical. Therefore, a

significant p-value means two materials have a statistically significant difference of responses in the given Stokes parameter. This test has the advantage of being non-parametric and therefore does not require the normality assumptions necessary for classical ANOVA.

3 Results

3.1 Michelson contrast findings

The Michelson contrast results suggest the polarimetric and derived Stokes parameters (S1, S2, DOLP, AOP, and ETM) provide necessary information to distinguish between similar and different materials when materials are otherwise too similar using the unpolarized panchromatic band (S0) to differentiate them. We analyzed the VIS, SWIR, and LWIR bands separately and found that the SWIR was most consistent in distinguishing between materials.

Michelson contrast results of same materials showed that the notch of polarimetric and derived Stokes parameters were more likely to overlap with the notch of the unpolarized Stokes parameter than when compared to different materials (Figure 7). Because they are the same materials, we expected the polarimetric Stokes parameter contrast notches to overlap with the S0 notches, which the data demonstrated (Table 4*a*–*c*).

When comparing different materials to each other, the notch of the polarimetric and derived Stokes parameters were less likely to overlap with the notch of the S0 (Figure 8). When the notch of the polarimetric and derived Stokes parameters do not overlap with the unpolarized Stokes parameter, it suggests that the polarized and derived Stokes parameters may provide a more robust spectropolarimetric signature to distinguish between the materials (Table 5*a*–*c*).

We examined whether the boxplots overlapped with a Michelson value of zero for each Stokes parameter to determine the amount of similarity between materials and found a high degree of overlap between same materials (i.e., building polygons to other building polygons) across Stokes parameters in the VIS and SWIR (Table 6*a*–*c*). When comparing different materials by examining whether the boxplots overlapped with a Michelson value of zero, we found materials with a low degree of overlap over zero across all of the Stokes parameters in the VIS, in the S0 and ETM in the SWIR, and DOLP and ETM in the LWIR.

The Michelson contrast values were most often at or near zero when comparing same materials, suggesting same materials are

indistinguishable from each other and thus their spectropolarimetric values may be used to create signatures (Figure 7). Likewise, different materials often showed high contrast to each other using the Michelson contrast (their values in the boxplot are less likely to overlap with zero, due to their higher contrast) (Figure 8).

Table 4*a–c*. Percent of notches in the boxplots from the Michelson contrasts in the VIS, SWIR, and LWIR for the polarimetric and derived Stokes parameters (S1, S2, DOLP, AOP, and ETM) that overlap with the unpolarized (S0) Michelson Contrast notches for same material comparisons. The cells were highlighted when all of the polygon ROIs for a polarimetric or derived Stokes parameter overlapped with S0.

(a) Grand Junction and Spanish Fork combined VIS result.

Same Material Comparison	Total for each parameter	% times S0 same as S1	% times S0 same as S2	% times S0 same as DOLP	% times S0 same as AOP	% times S0 same as ETM
Road-comparison	8	62.50	87.50	75.00	87.50	75.00
Building-comparison	7	100.00	100.00	100.00	100.00	100.00
Car-comparison	5	80.00	80.00	80.00	80.00	100.00
Scrub-comparison	5	60.00	60.00	60.00	40.00	80.00
Fallow agriculture—comparison	3	100.00	0.00	33.33	66.67	100.00
GrassField—comparison	3	66.67	100.00	100.00	66.67	100.00
Tree-comparison	1	100.00	100.00	100.00	100.00	100.00

(b) Grand Junction and Spanish Fork combined SWIR result.

Same Material Comparison	Total for each parameter	% times S0 same as S1	% times S0 same as S2	% times S0 same as DOLP	% times S0 same as AOP	% times S0 same as ETM
Road-comparison	8	75.00	87.50	87.50	75.00	87.50
Building-comparison	7	85.71	100.00	100.00	100.00	100.00
Car-comparison	5	80.00	100.00	100.00	60.00	100.00
Scrub-comparison	5	60.00	80.00	100.00	80.00	100.00
Fallow Agriculture-comparison	3	33.33	100.00	100.00	66.67	100.00
GrassField-comparison	3	66.67	100.00	100.00	100.00	100.00
Tree-comparison	1	100.00	100.00	100.00	100.00	100.00

(c) Grand Junction and Spanish Fork combined LWIR result.

Same Material Comparison	Total for each parameter	% times S0 same as S1	% times S0 same as S2	% times S0 same as DOLP	% times S0 same as AOP	% times S0 same as ETM
Road-comparison	8	75.00	75.00	50.00	62.50	87.50
Building-comparison	7	71.43	57.14	57.14	71.43	57.14
Car-comparison	5	40.00	60.00	60.00	80.00	100.00
Scrub-comparison	5	60.00	60.00	80.00	40.00	60.00
Fallow Agriculture-comparison	3	66.67	33.33	66.67	66.67	100.00
GrassField-comparison	3	33.33	100.00	66.67	66.67	66.67
Tree-comparison	1	0.00	100.00	0.00	100.00	100.00

Table 5*a–c*. Percent of notches in the boxplots from the Michelson contrasts in the VIS, SWIR, and LWIR for the polarimetric and derived Stokes parameters (S1, S2, DOLP, AOP, and ETM) that overlap with the unpolarized (S0) Michelson Contrast notches for different feature comparisons. The highlighted cells show when all of the polygon ROIs for a polarimetric or derived Stokes parameter did not overlap with S0, suggesting that the polarimetric or derived Stokes parameters contained more information than the S0.

(a) Grand Junction and Spanish Fork combined VIS result.

Different Material Comparison	Total for each parameter	% times S0 different from S1	% times S0 different from S2	% times S0 different from DOLP	% times S0 different from AOP	% times S0 different from ETM
Building—Road	7	85.71	85.71	85.71	71.43	71.43
Building—Scrub	5	80.00	80.00	80.00	80.00	20.00
Road—Scrub	5	100.00	100.00	100.00	100.00	60.00
Car—Road	5	100.00	100.00	100.00	100.00	60.00
Car—Building	4	75.00	75.00	100.00	75.00	50.00
Car—Scrub	3	100.00	100.00	100.00	100.00	0.00
Road—GrassField	3	100.00	100.00	100.00	100.00	66.67
GrassField—Building	3	33.33	100.00	100.00	66.67	66.67
Fallow Agriculture—Road	3	100.00	100.00	100.00	100.00	100.00
Fallow Agriculture—Building	2	100.00	0.00	0.00	100.00	0.00
Fallow Agriculture—Car	1	100.00	100.00	100.00	100.00	100.00
Fallow Agriculture—Scrub	1	100.00	100.00	100.00	100.00	0.00
Fallow Agriculture—GrassField	1	0.00	0.00	0.00	0.00	0.00
Road—Tree	1	100.00	100.00	100.00	100.00	100.00
Tree—Car	1	100.00	100.00	100.00	100.00	100.00
Tree—Fallow Agriculture	1	100.00	100.00	100.00	100.00	100.00
GrassField—Car	1	100.00	100.00	100.00	100.00	100.00
Scrub—GrassField	1	100.00	100.00	100.00	100.00	0.00

(b) Grand Junction and Spanish Fork combined SWIR result.

Different Material Comparison	Total for each parameter	% times S0 different from S1	% times S0 different from S2	% times S0 different from DOLP	% times S0 different from AOP	% times S0 different from ETM
Building—Road	7	57.14	57.14	100.00	14.29	14.29
Building—Scrub	5	80.00	100.00	100.00	60.00	20.00
Road—Scrub	5	80.00	100.00	100.00	80.00	0.00
Car—Road	5	80.00	60.00	60.00	20.00	40.00
Car—Building	4	50.00	75.00	75.00	25.00	0.00
Car—Scrub	3	66.67	66.67	100.00	66.67	0.00
Road—GrassField	3	100.00	66.67	100.00	66.67	0.00
GrassField—Building	3	33.33	66.67	66.67	66.67	0.00
Fallow Agriculture—Road	3	33.33	66.67	100.00	100.00	0.00
Fallow Agriculture—Building	2	50.00	100.00	100.00	100.00	0.00
Fallow Agriculture—Car	1	100.00	0.00	100.00	100.00	0.00
Fallow Agriculture—Scrub	1	100.00	100.00	100.00	100.00	0.00
Fallow Agriculture—GrassField	1	100.00	100.00	100.00	100.00	0.00
Road—Tree	1	100.00	0.00	0.00	0.00	0.00
Tree—Car	1	100.00	0.00	0.00	0.00	0.00
Tree—Fallow Agriculture	1	0.00	100.00	100.00	100.00	0.00
GrassField—Car	1	100.00	100.00	100.00	0.00	0.00
Scrub—GrassField	1	0.00	0.00	100.00	0.00	0.00

(c) Grand Junction and Spanish Fork combined LWIR result.

Different Material Comparison	Total for each parameter	% times S0 different from S1	% times S0 different from S2	% times S0 different from DOLP	% times S0 different from AOP	% times S0 different from ETM
Building—Road	7	28.57	57.14	42.86	28.57	42.86
Building—Scrub	5	60.00	60.00	40.00	60.00	40.00
Road—Scrub	5	40.00	60.00	40.00	20.00	20.00
Car—Road	5	40.00	0.00	80.00	40.00	100.00
Car—Building	4	75.00	25.00	25.00	50.00	75.00
Car—Scrub	3	0.00	100.00	66.67	66.67	66.67
Road—GrassField	3	0.00	66.67	66.67	33.33	33.33
GrassField—Building	3	66.67	100.00	66.67	66.67	33.33
Fallow Agriculture—Road	3	100.00	66.67	33.33	66.67	100.00
Fallow Agriculture—Building	1	0.00	100.00	0.00	0.00	0.00
Fallow Agriculture—Car	1	100.00	100.00	100.00	100.00	100.00
Fallow Agriculture—Scrub	1	0.00	0.00	100.00	100.00	0.00
Fallow Agriculture—GrassField	1	0.00	0.00	0.00	0.00	0.00

Different Material Comparison	Total for each parameter	% times S0 different from S1	% times S0 different from S2	% times S0 different from DOLP	% times S0 different from AOP	% times S0 different from ETM
Road—Tree	1	100.00	100.00	100.00	100.00	100.00
Tree—Car	1	100.00	100.00	100.00	100.00	100.00
Tree—Fallow Agriculture	1	100.00	0.00	100.00	0.00	100.00
GrassField—Car	1	0.00	0.00	100.00	0.00	100.00
Scrub—GrassField	1	100.00	100.00	100.00	100.00	100.00

Table 6*a–c*. Percent of boxplots that overlap with a Michelson contrast value of zero. A high percentage of boxplots that overlap with zero indicate low contrast between materials, suggesting the materials are either the same, similar, or not differentiable. A low percentage of boxplots that overlap with zero indicate high contrast between materials, suggesting the materials are different or are not differentiable from each other. Boxes highlighted in yellow under "Same material comparison" show that the materials' boxplots all overlapped with zero, while boxes highlighted in orange show that the materials' boxplots overlapped with zero at a rate ranging from 75–99%. Boxes highlighted in yellow under "Different material comparison" show that no materials' boxplots overlapped with zero, while boxes highlighted in orange show that the materials' boxplots overlapped with zero at a rate between 1–25%.

(a) Grand Junction and Spanish Fork combined VIS result.

Same material comparison	Total for each parameter	S0	S1	S2	DOLP	AOP	ETM
Road—comparison	8	75.00%	62.50%	87.50%	87.50%	62.50%	87.50%
Building—comparison	7	85.71%	100.00%	100.00%	85.71%	100.00%	85.71%
Car—comparison	5	60.00%	40.00%	60.00%	60.00%	100.00%	80.00%
Scrub—comparison	5	80.00%	80.00%	80.00%	80.00%	100.00%	80.00%
Fallow Agriculture—comparison	3	33.33%	100.00%	33.33%	33.33%	100.00%	33.33%
GrassField—comparison	3	100.00%	66.67%	100.00%	100.00%	33.33%	100.00%
Tree—comparison	1	100.00%	100.00%	100.00%	100.00%	100.00%	100.00%
Different material comparison	**Total for each parameter**	**S0**	**S1**	**S2**	**DOLP**	**AOP**	**ETM**
Road—Building	7	28.57%	14.29%	14.29%	14.29%	28.57%	28.57%
Building—Scrub	5	40.00%	40.00%	20.00%	40.00%	0.00%	40.00%
Road—Scrub	5	0.00%	0.00%	0.00%	0.00%	20.00%	0.00%
Car—Road	5	0.00%	20.00%	0.00%	0.00%	40.00%	0.00%
Car—Building	4	0.00%	75.00%	25.00%	50.00%	100.00%	0.00%
Car—Scrub	3	0.00%	33.33%	66.67%	0.00%	100.00%	0.00%
Road—GrassField	3	0.00%	0.00%	0.00%	0.00%	0.00%	0.00%
GrassField—Building	3	0.00%	66.67%	0.00%	0.00%	33.33%	0.00%
FallowAgriculture—Road	3	0.00%	0.00%	0.00%	0.00%	0.00%	0.00%
Fallow Agriculture—Building	2	100.00%	0.00%	50.00%	50.00%	0.00%	100.00%
Fallow Agriculture—Car	1	0.00%	0.00%	0.00%	0.00%	0.00%	0.00%
Fallow Agriculture—Scrub	1	0.00%	0.00%	0.00%	0.00%	100.00%	0.00%
Fallow Agriculture—GrassField	1	0.00%	100.00%	0.00%	0.00%	0.00%	0.00%
Road—Tree	1	0.00%	0.00%	0.00%	0.00%	0.00%	0.00%

Different material comparison	Total for each parameter	S0	S1	S2	DOLP	AOP	ETM
Tree—Car	1	0.00%	0.00%	0.00%	0.00%	0.00%	0.00%
Tree—Fallow Agriculture	1	0.00%	0.00%	0.00%	0.00%	0.00%	0.00%
GrassField—Car	1	0.00%	0.00%	100.00%	100.00%	100.00%	0.00%
Scrub—GrassField	1	100.00%	0.00%	0.00%	100.00%	0.00%	100.00%

(b) Grand Junction and Spanish Fork combined SWIR result.

Same material comparison	Total for each parameter	S0	S1	S2	DOLP	AOP	ETM
Road—comparison	8	87.50%	87.50%	75.00%	100.00%	62.50%	87.50%
Building—comparison	7	85.71%	100.00%	100.00%	85.71%	100.00%	85.71%
Car—comparison	5	100.00%	80.00%	100.00%	80.00%	80.00%	40.00%
Scrub—comparison	5	100.00%	80.00%	80.00%	80.00%	80.00%	100.00%
Fallow Agriculture—comparison	3	100.00%	33.33%	100.00%	100.00%	66.67%	100.00%
GrassField—comparison	3	100.00%	66.67%	100.00%	100.00%	100.00%	100.00%
Tree—comparison	1	100.00%	100.00%	100.00%	100.00%	100.00%	100.00%
Different material comparison	**Total for each parameter**	**S0**	**S1**	**S2**	**DOLP**	**AOP**	**ETM**
Road—Building	7	28.57%	71.43%	71.43%	71.43%	85.71%	14.29%
Building—Scrub	5	0.00%	40.00%	60.00%	20.00%	40.00%	0.00%
Road—Scrub	5	0.00%	40.00%	20.00%	20.00%	20.00%	0.00%
Car—Road	5	0.00%	20.00%	80.00%	20.00%	60.00%	0.00%
Car—Building	4	0.00%	50.00%	75.00%	25.00%	50.00%	0.00%
Car—Scrub	3	33.33%	0.00%	33.33%	0.00%	66.67%	66.67%
Road—GrassField	3	0.00%	100.00%	33.33%	33.33%	66.67%	0.00%
GrassField—Building	3	33.33%	33.33%	66.67%	33.33%	100.00%	0.00%
FallowAgriculture—Road	3	0.00%	100.00%	33.33%	33.33%	66.67%	0.00%
Fallow Agriculture—Building	2	0.00%	100.00%	0.00%	0.00%	100.00%	0.00%
Fallow Agriculture—Car	1	100.00%	100.00%	200.00%	100.00%	100.00%	100.00%
Fallow Agriculture—Scrub	1	0.00%	0.00%	0.00%	0.00%	0.00%	0.00%
Fallow Agriculture—GrassField	1	0.00%	0.00%	0.00%	0.00%	0.00%	0.00%
Road—Tree	1	0.00%	100.00%	100.00%	0.00%	100.00%	0.00%
Tree—Car	1	0.00%	0.00%	100.00%	0.00%	0.00%	0.00%

Different material comparison	Total for each parameter	S0	S1	S2	DOLP	AOP	ETM
Tree—Fallow Agriculture	1	0.00%	100.00%	0.00%	0.00%	100.00%	0.00%
GrassField—Car	1	0.00%	0.00%	0.00%	100.00%	100.00%	0.00%
Scrub—GrassField	1	0.00%	100.00%	100.00%	0.00%	100.00%	0.00%

(c) Grand Junction and Spanish Fork combined LWIR result.

Same material comparison	Total for each parameter	S0	S1	S2	DOLP	AOP	ETM
Road—comparison	8	87.50%	75.00%	62.50%	50.00%	62.50%	87.50%
Building—comparison	7	85.71%	71.43%	57.14%	57.14%	71.43%	71.43%
Car—comparison	5	100.00%	60.00%	60.00%	80.00%	100.00%	100.00%
Scrub—comparison	5	100.00%	60.00%	60.00%	80.00%	40.00%	60.00%
Fallow Agriculture—comparison	3	100.00%	66.67%	33.33%	66.67%	100.00%	66.67%
GrassField—comparison	3	66.67%	100.00%	100.00%	100.00%	66.67%	66.67%
Tree—comparison	1	100.00%	100.00%	100.00%	0.00%	100.00%	100.00%

Different material comparison	Total for each parameter	S0	S1	S2	DOLP	AOP	ETM
Road—Building	7	42.86%	28.57%	85.71%	0.00%	57.14%	14.29%
Building—Scrub	5	0.00%	60.00%	60.00%	0.00%	60.00%	0.00%
Road—Scrub	5	100.00%	40.00%	60.00%	20.00%	60.00%	20.00%
Car—Road	5	100.00%	80.00%	80.00%	0.00%	40.00%	20.00%
Car—Building	4	25.00%	50.00%	50.00%	75.00%	75.00%	25.00%
Car—Scrub	3	100.00%	100.00%	66.67%	0.00%	66.67%	0.00%
Road—GrassField	3	66.67%	66.67%	100.00%	33.33%	66.67%	0.00%
GrassField—Building	3	33.33%	33.33%	66.67%	33.33%	100.00%	0.00%
FallowAgriculture—Road	3	66.67%	100.00%	33.33%	0.00%	66.67%	33.33%
Fallow Agriculture—Building	3	100.00%	0.00%	50.00%	0.00%	0.00%	50.00%
Fallow Agriculture—Car	1	0.00%	100.00%	0.00%	0.00%	0.00%	0.00%
Fallow Agriculture—Scrub	1	100.00%	0.00%	0.00%	100.00%	100.00%	0.00%
Fallow Agriculture—GrassField	1	100.00%	0.00%	0.00%	0.00%	0.00%	0.00%
Road—Tree	1	0.00%	0.00%	0.00%	100.00%	0.00%	0.00%
Tree—Car	1	0.00%	0.00%	0.00%	0.00%	0.00%	0.00%

Different material comparison	Total for each parameter	S0	S1	S2	DOLP	AOP	ETM
Tree—Fallow Agriculture	1	100.00%	100.00%	100.00%	100.00%	100.00%	100.00%
GrassField—Car	1	0.00%	100.00%	100.00%	0.00%	100.00%	0.00%
Scrub—GrassField	1	100.00%	100.00%	100.00%	100.00%	100.00%	100.00%

Figure 7. Michelson contrast results from the comparison of building ROI polygons to each other in the VIS in one scene in Grand Junction, CO. The notches of the S1, S2, DOLP, AOP, and ETM overlap with the S0, indicating the polarimetric and derived Stokes parameters provide no additional value in identifying buildings as separate materials from each other. Additionally, the Michelson contrast values overlap with zero, indicating low to no contrast between other building ROIs, further suggesting the building ROIs are distinct from other materials.

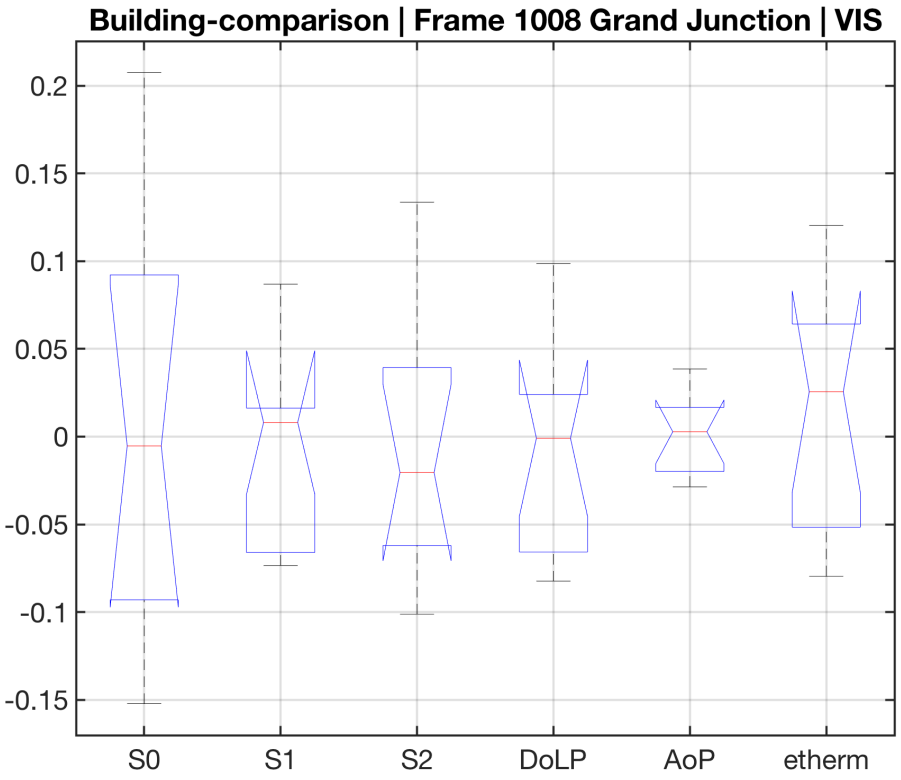

Figure 8. Michelson contrast results comparing road and building ROI polygons in the VIS in one scene in Grand Junction, CO. The notches of the S1, S2, DOLP, and ETM do not overlap with the S0, indicating these polarimetric and derived Stokes parameters provide additional value in differentiating between roads and buildings.

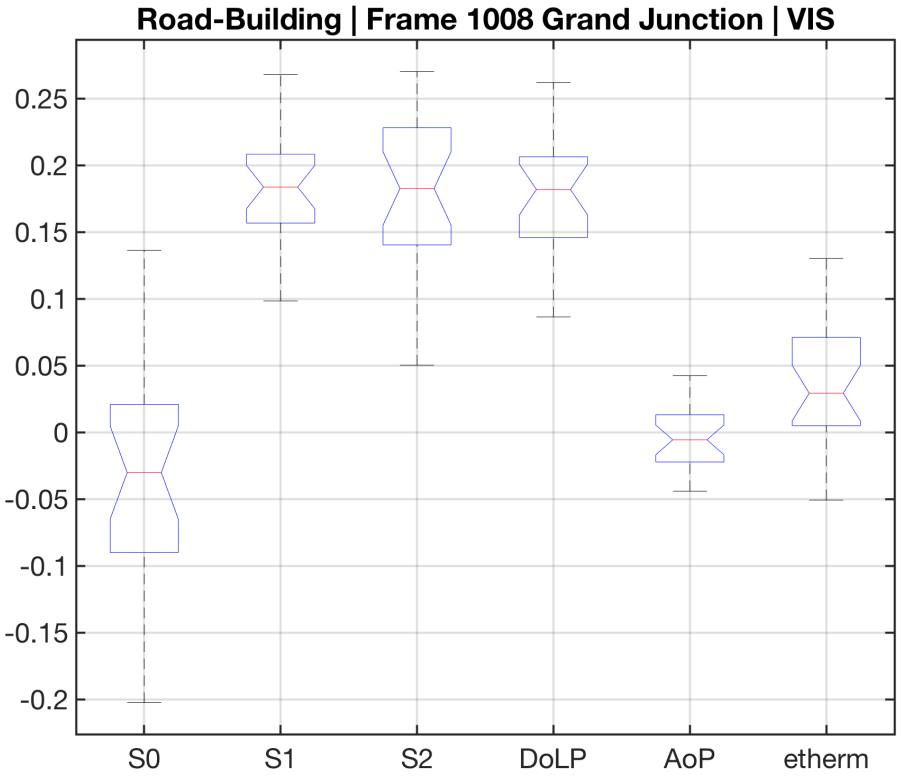

3.2 ANOVA findings

Results from the Kruskal-Wallis one-way ANOVA H-test showed that the following Stokes parameters can be used to differentiate between various manmade materials: the S0, S1, S2, DOLP, AOP, and ETM in the VIS; the S0, S1, and ETM in the SWIR; and the S0, S1, DOLP, and ETM in the LWIR. Results showed that the following Stokes parameters can be used to differentiate between various natural materials: the S0 in the VIS; S0, S1, and AOP in the SWIR; and the S2 and ETM in the LWIR. (Table 7*a*–*c*).

We applied the ANOVA technique to the two study sites after we combined them and found that fewer materials maintained statistical significance from each other compared to when analyzing the sites individually, which could be because the scenes were not calibrated to each other, materials differed too much by study site, differences in camera collection angle, or

variations in image acquisition time of day. However, we still found that similar materials were differentiable when combining the two sites together (Table 7*c*).

We summarized Stokes parameters to show each band where natural materials are differentiable from natural materials or where manmade materials are differentiable from other manmade materials (Table 8). The unpolarized S0 in the VIS, SWIR, and LWIR at each site exhibited a high degree of efficacy in discriminating between similar manmade materials. Upon examination of the polarimetric and derived Stokes parameter results, manmade materials were most differentiable in the VIS most consistently. The ETM in the LWIR most consistently exhibited the ability to discriminate manmade from other manmade materials. Otherwise, some Stokes parameters at different bands at one study site (i.e., manmade in the S1 LWIR in Grand Junction, CO, but not in Spanish Fork, UT) exhibited success in discriminating between similar materials, but the same result was not consistently replicated in the other study site.

Table 7*a–c*. Results from ANOVA testing showing the materials that exhibit statistically significant difference by wavelength and Stokes parameter at each study site and aggregated across both study sites in this research.

(a) Materials that exhibit statistically significant difference at the Spanish Fork, UT, site.

Stokes Parameter	VIS	SWIR	LWIR
S0	Road—Scrub Road—Building Road—GrassField Road—FallowAgriculture Road—Car Scrub—Car Building—Car	Road—Scrub Road—Car Road—FallowAgriculture Road—GrassField Building—FallowAgriculture Building—GrassField	Scrub—Road Scrub—FallowAgriculture Scrub—Building GrassField—Building Car—Building Road—Building
S1	Road—FallowAgriculture Road—Scrub Road—GrassField Car—GrassField Building—Scrub Building—GrassField	FallowAgriculture—Scrub FallowAgriculture—GrassField	Road—Scrub Road—Building Road—GrassField
S2	Road—Scrub Road—FallowAgriculture Road—GrassField Road—Car Building—GrassField Building—Car	Road—Scrub Road—GrassField Building—Scrub Building—GrassField	GrassField—FallowAgriculture

Stokes Parameter	VIS	SWIR	LWIR
DOLP	Car—Building Car—Road GrassField—Building GrassField—Road FallowAgriculture—Road Scrub—Road	GrassField—Road GrassField—Building GrassField—Car Scrub—Road Scrub—Building Scrub—Car FallowAgriculture—Car	Road—Car Road—Building Scrub—Building FallowAgriculture—Building
AOP	Road—FallowAgriculture Road—Scrub Road—GrassField Building—Scrub Building—GrassField	FallowAgriculture—Scrub FallowAgriculture—GrassField Road—Scrub Road—GrassField Building—Scrub Building—GrassField	-
ETM	Road—Building Road—GrassField Road—FallowAgriculture Road—Car Scrub—Car	Road—Scrub Road—FallowAgriculture Road—GrassField Building—Scrub Building—FallowAgriculture Building—GrassField	Scrub—FallowAgriculture Scrub—Road Scrub—Building GrassField—Road GrassField—Building Car—Building

(b) Materials that exhibit statistically significant difference at the Grand Junction, CO, site.

Stokes Parameter	VIS	SWIR	LWIR
S0	Tree—Building Tree—Car Road—Scrub Road—Building Road—Car FallowAgriculture—Car	Road—FallowAgriculture Road—Car Road—GrassField Building—Car Building—GrassField	FallowAgriculture—Road FallowAgriculture—Building Tree—Road Tree—Building GrassField—Road GrassField—Building Car—Building Scrub—Building Road—Building
S1	FallowAgriculture—Road Car—Road	Car—Road Car—Building	-
S2	Road—Car Road—Tree Road—GrassField Road—FallowAgriculture	Car—GrassField Building—GrassField	-

Stokes Parameter	VIS	SWIR	LWIR
DOLP	FallowAgriculture—Road Car—Road	FallowAgriculture—Car GrassField—Car	FallowAgriculture—Building FallowAgriculture—Car GrassField—Building GrassField—Car Tree—Building Tree—Car Road—Building Road—Car
AOP	Road—Car Road—Building Road—Scrub	Car—FallowAgriculture Car—GrassField Building—GrassField	-
ETM	Road—Building Road—Scrub Road—Car Tree—Car	Road—GrassField Road—FallowAgriculture Road—Car Road—Scrub Building—Car Building—Scrub	FallowAgriculture—Scrub FallowAgriculture—Road FallowAgriculture—Building Tree—Scrub Tree—Road Tree—Building GrassField—Road GrassField—Building Car—Road Car—Building

(c) Materials that exhibit statistically significant difference at Spanish Fork, UT, and Grand Junction, CO.

Stokes Parameter	VIS	SWIR	LWIR
S0	Tree—Scrub Tree—Building Tree—GrassField Tree—FallowAgriculture Tree—Car Road—Scrub Road—Building Road—GrassField Road—FallowAgriculture Road—Car Scrub—Car Building—Car	Road—Scrub Road—Car Road—FallowAgriculture Road—GrassField Building—Scrub Building—Car Building—FallowAgriculture Building—GrassField Scrub—GrassField	Tree—Road Tree—Building GrassField—Car GrassField—Road GrassField—Building FallowAgriculture—Building Scrub—Building Car—Building Road—Building
S1	-	FallowAgriculture—Road	Road—Scrub Road—Building Road—GrassField
S2	Road—Scrub Road—FallowAgriculture Road—GrassField Road—Car Road—Tree Building—GrassField Building—Car	Road—GrassField Building—GrassField	-

Stokes Parameter	VIS	SWIR	LWIR
	Scrub—Car		
DOLP	Tree—Road GrassField—Building GrassField—Road Car—Building Car—Road FallowAgriculture—Building FallowAgriculture—Road Scrub—Road Building—Road	GrassField—Road GrassField—Building GrassField—Car Scrub—Road Scrub—Building Scrub—Car FallowAgriculture—Road FallowAgriculture—Building FallowAgriculture—Car	Tree—Car Tree—Building Road—Car Road—Building FallowAgriculture—Car FallowAgriculture—Building GrassField—Car GrassField—Building Scrub—Car Scrub—Building
AOP	Road—Car Building—Car	-	-
ETM	Road—Scrub Road—Building Road—GrassField Road—FallowAgriculture Road—Car Tree—Car Scrub—Car Building—Car GrassField—Car	Road—Scrub Road—Car Road—FallowAgriculture Road—GrassField Building—Scrub Building—Car Building—FallowAgriculture Building—GrassField	Tree—Road Tree—Building GrassField—Road GrassField—Building Car—Road Car—Building Scrub—Road Scrub—Building FallowAgriculture—Building Road—Building

Table 8. Stokes parameters at each band where natural materials exhibit statistical significance from other natural materials or where manmade materials exhibit statistical significance from other manmade materials.

Spanish Fork, UT			
Stokes Parameter	**VIS**	**SWIR**	**LWIR**
S0	Manmade	Manmade	Manmade
S1	-	Natural	Manmade
S2	Manmade	-	Natural
DOLP	Manmade	-	Manmade
AOP	-	Natural	-
ETM	Manmade	-	Manmade, natural
Grand Junction, CO			
Stokes Parameter	**VIS**	**SWIR**	**LWIR**
S0	Manmade	Manmade	Manmade
S1	Manmade	Manmade	-
S2	Manmade	-	-
DOLP	Manmade	-	Manmade
AOP	Manmade	-	-
ETM	Manmade	Manmade	Manmade, natural
Spanish Fork, UT and Grand Junction, CO			
Stokes Parameter	**VIS**	**SWIR**	**LWIR**
S0	Manmade, natural	Manmade, natural	Manmade
S1	-	-	Manmade
S2	Manmade	-	-
DOLP	Manmade	-	Manmade
AOP	Manmade	-	-
ETM	Manmade	Manmade	Manmade

4 Discussion

Prior research has focused on using spectropolarimetric imagery for anomaly detection in identifying manmade materials in natural backgrounds. Our approach focuses on identifying materials with spectral reflectances that are similar, such as similar manmade or natural features in a scene. Bartlett et al. (2011) used a sensor that collected single-band 450–720 nm spectropolarimetric imagery to find multiple vehicles in a model desert scene using an anomaly detection model based on Mahalanobis and Euclidean distances. In this study, the authors stacked the S0, S1, and S2 Stokes parameters using a scaling approach to constrain S0 to the same relative data range as S1 and S2. This approach was highly accurate at target identification. Aron and Gronau (2005) tested spectropolarimetric imagery in the midwave infrared and LWIR to detect a vehicle and tent among a natural background. Our approach differed from theirs in that we focused on differentiating between similar materials using a pairwise comparison approach comparing individual Stokes parameters at individual bands, and we found similarities between materials that were either the same or similar, both using the Michelson contrast and the ANOVA statistic.

The Stokes parameters and bands were not stacked into hypercubes because the values of the S0 are higher than those of the other Stokes parameters and would overwhelm the signature and skew the ability to determine separability. The layer stacking approach using scaling by Bartlett et al. (2011) would provide a technique to combine the imagery to create a hypercube to determine separability of all materials in a scene.

In our study, we determined material separability using contrast and statistical approaches. Recent research has shown that discrimination may be enhanced by using a metric that is more inclusive of target and background data. This approach combines multiple metrics, including the Michelson contrast (Pezzaniti et al. 2021). Future research may explore the new multiple metric approach in addition to use of distance and machine-learning approaches to map multiple materials in a scene using spectropolarimetric imagery as well as a development of a binary mapping approach when interested in just one material while excluding all other

materials. Use of machine learning and binary approaches using VIR spectral imagery has been a focus of GRL.

Additionally, future research may focus on calibrating the imagery to aid with creating reliable signatures that maintain consistency in multiple images and on using the cameras to collect data in the laboratory of different materials at different angles to determine if there is an optimal angle. We would vary directions of view and illumination with which the cameras collect the data and incorporate the information as signature attributes to determine if these differences could affect the separability of materials. Models essential to this effort will be developed based upon the approach of Meng and Kerekes (2011) in order to better understand the advantages and limitations of the VIS, SWIR, and LWIR cameras. Meng and Kerekes (2011) compared image to sample data by calculating the root mean square error between the image and sample data Stokes parameters calculated by each instrument.

5 Conclusion

This study employed contrast and statistical methodologies using VIS, SWIR, and LWIR spectropolarimetric imagery to determine if similar materials could be differentiated with the addition of polarimetric and derived Stokes parameters. This study shows the addition of polarimetric data is especially useful when data are otherwise too similar to differentiate. The study used the Michelson contrast and ANOVA to compare materials identified in imagery collected over Spanish Fork, UT, and Grand Junction, CO. The technique showed that spectropolarimetric imagery can be used to differentiate between similar materials, which has previously focused on identifying materials that had high contrast with their backgrounds.

References

Aron, Y., and Y. Gronau. 2005. “Polarization in the LWIR: A Method to Improve Target Acquisition.” *Infrared Technology and Applications XXXI* 5783: 653–61. Bellingham, WA: International Society for Optics and Photonics.

Bartlett, B. D., A. Schlamm, C. Salvaggio, and D. W. Messinger. 2011. “Anomaly Detection of Man-made Objects Using Spectropolarimetric Imagery.” *Algorithms and Technologies for Multispectral, Hyperspectral, and Ultraspectral Imagery XVII* 8048: 80480B. Bellingham, WA: International Society for Optics and Photonics.

Becker, S.J., C. S. T. Daughtry, and A. L. Russ. 2018. “Robust Forest Cover Indices for Multispectral Images.” *Photogrammetric Engineering and Remote Sensing* 84 (8): 505–512. doi: https://10.14358/PERS.84.8.505.

Bright, C., F. Pantuso, and J. Zadnik. 2019. U.S. Army Combat Capabilities Development Command—C5ISR Center, Polarization Effort Status.

Chambers, J. M., W. S. Cleveland, B. Kleiner, and P. A. Tukey. 1983. "Comparing Data Distributions." *Graphical Methods for Data Analysis* 62. Belmont, CA: Wadsworth International Group.

Chenault, D., L. Pezzaniti, J. Vaden, M. Roche, J. Michalson, and K. Gurton. 2015. *Pyxis: Enhanced Thermal Imaging with a Division of Focal Plane Polarimeter*. Technical Report, Polaris Sensor Technologies, Inc.

Gurton, K. P., and M. Felton. 2009. “Detection of Disturbed Earth Using Passive LWIR Polarimetric Imaging.” *Polarization Science and Remote Sensing IV* 7461: 746115. Bellingham, WA: International Society for Optics and Photonics. doi: 10.1117/12.837779.

Herold, M., M. Gardner, B. Hadley, and D. Roberts. 2002. “The Spectral Dimension in Urban Land Cover Mapping from High-Resolution Optical Remote Sensing Data. In *Proceedings of the 3rd Symposium on Remote Sensing of Urban Areas* (Vol. 6, p. 2002).

Können, G. P. 1985. *Polarized Light in Nature*. New York: Cambridge University Press.

Kruskal, W. H., and W. A. Wallis. 1952. “Use of Ranks in One-Criterion Variance Analysis.” *Journal of the American Statistical Association* 47 (260): 583–621. doi: 10.1080/01621459.1952.10483441.

Lavigne, D. A., M. Breton, G. Fournier, M. Pichette, and V. Rivet. 2009. “Development of Performance Metrics to Characterize the Degree of Polarization of Man-made Objects Using Passive Polarimetric Images.” *Signal Processing, Sensor Fusion, and Target Recognition XVIII* 7336: 73361A. Bellingham, WA: International Society for Optics and Photonics. doi: 10.1117/12.819020.

Meng, L., and J. P. Kerekes. 2011. “Analytical Modeling of Optical Polarimetric Imaging Systems.” *2011 IEEE International Geoscience and Remote Sensing Symposium*: 3998–4001. doi: 10.1109/IGARSS.2011.6050108.

Michelson, A. A. 1927. *Studies in Optics*. Chicago: University of Chicago Press.

Myint, S. W., P. Gober, A. Brazel, S. Grossman-Clarke, and Q. Weng. 2011. "Per-pixel vs. Object-based Classification of Urban Land Cover Extraction Using High Spatial Resolution Imagery." *Remote Sensing of Environment* 115 (5): 1145–61. doi: 10.1016/j.rse.2010.12.017.

Pantuso, F. P., C. J. Bright, M. Polcha, J. C. Shpil, and A. S. Lapointe. 2018. *Long Wave Infrared (LWIR) Polarization for Enhanced Detection of Surface Hazards in Cluttered Scenes*. Report for the Night Vision and Electronic Sensors Directorate.

Pezzaniti, J. L., I. Semyonov, F. P. Pantuso, J. A. Zadnik, C. J. Bright, and D. Chenault. 2021. "A New Metric for Describing 'Visibility' in an Image." *Battlefield Survivability and Discrimination* (August). Orlando, FL: Military Sensing Symposia.

Shapiro, S. S., and M. B. Wilk. 1965. "An Analysis of Variance Test for Normality (Complete Samples)." *Biometrika* 52 (3/4): 591–611.

Tyo, J. S., D. H. Goldstein, D. B. Chenault, and J. A. Shaw. 2006. "Review of Passive Imaging Polarimetry for Remote Sensing Applications." *Applied Optics* 45: 5453–69.

Vanderbilt, V., C. Daughtry, and R. Dahlgren. 2019. "Polarization to Estimate Leaf Surface Reflectance." Proc. SPIE 11132, *Polarization Science and Remote Sensing IX* 11132: 1113205. doi: 10.1117/12.2529214.

Zhou, P.C., F. Wang, H. K. Zhang, and M. G. Xue. 2011. "Camouflaged Target Detection Based on Visible and Near Infrared Polarimetric Imagery Fusion. *International Symposium on Photoelectronic Detection and Imaging 2011: Advances in Imaging Detectors and Applications* 8194: 81940Y. Bellingham, WA: International Society for Optics and Photonics. doi: 10.1117/12.899590.

REPORT DOCUMENTATION PAGE

Form Approved
OMB No. 0704-0188

1. REPORT DATE (DD-MM-YYYY)	2. REPORT TYPE	3. DATES COVERED (From - To)
09-2022	Final	

4. TITLE AND SUBTITLE
Analysis of Spectropolarimetric Responses in the Visible and Infrared for Differentiation between Similar Materials

5a. CONTRACT NUMBER

5b. GRANT NUMBER

5c. PROGRAM ELEMENT
611102

6. AUTHOR(S)
Sarah J. Becker, Heather S. Sussman, S. Bruce Blundell, Vern C. Vanderbilt, and Igor Semyonov

5d. PROJECT NUMBER
AB2

5e. TASK NUMBER

5f. WORK UNIT NUMBER

7. PERFORMING ORGANIZATION NAME(S) AND ADDRESS(ES)
US Army Engineer Research and Development Center (ERDC)
Geospatial Research Laboratory (GRL)
7701 Telegraph Road
Alexandria, VA 22315-3864

8. PERFORMING ORGANIZATION REPORT NUMBER
ERDC/GRL-TR-22-2

9. SPONSORING / MONITORING AGENCY NAME(S) AND ADDRESS(ES)
Headquarters
US Army Corps of Engineers
441 G Street NW
Washington, DC 20314-1000

10. SPONSOR/MONITOR'S ACRONYM(S)

11. SPONSOR/MONITOR'S REPORT NUMBER(S)

12. DISTRIBUTION / AVAILABILITY STATEMENT
Approved for public release; distribution is unlimited.

13. SUPPLEMENTARY NOTES

14. ABSTRACT

Spectropolarimetric research has focused on target detections of materials that have a high degree of contrast from background materials, such as identification of a manmade object embedded in a vegetative background. This study presents an approach using spectropolarimetric imagery in visible, shortwave infrared, and longwave infrared bands to differentiate between similar natural and manmade materials. The method employs Michelson contrast and Kruskal-Wallis one-way analysis of variance (ANOVA) H-test to determine if a distinction can be found in pairwise comparisons of similar and different materials using the Stokes parameters in the visible, shortwave infrared, and longwave infrared bands. Results showed that similar natural and manmade materials were differentiable in spectropolarimetric imagery using the Michelson contrast and ANOVA. This approach provides a way to use spectropolarimetric imagery to distinguish between materials that are similar to each other.

15. SUBJECT TERMS
Spectropolarimetric remote sensing; Remote sensing images; Materials--Detection; Land cover--Detection

16. SECURITY CLASSIFICATION OF:			17. LIMITATION OF ABSTRACT	18. NUMBER OF PAGES	19a. NAME OF RESPONSIBLE PERSON
a. REPORT	b. ABSTRACT	c. THIS PAGE			19b. TELEPHONE NUMBER (include area code)
Unclassified	Unclassified	Unclassified	none	43	